

Hysteresis in a system driven by either generalized force or displacement variables

Erell Bonnot,¹ Ricardo Romero,^{1,2} Xavier Illa,¹ Lluís Mañosa,¹ Antoni Planes,¹ and Eduard Vives^{1,*}

¹ Departament d'Estructura i Constituents de la Matèria, Universitat de Barcelona

Diagonal 647, Facultat de Física, 08028 Barcelona, Catalonia

²IFIMAT. CICPBA and Universidad Nacional del Centro. Pinto 399, 7000 Tandil, Argentina

(Dated: May 26, 2019)

We report on experiments aimed at comparing the hysteretic response of a Cu-Zn-Al single crystal undergoing a martensitic transition under *strain-driven* and *stress-driven* conditions. *Strain-driven* experiments were performed using a conventional tensile machine while a special device was designed to perform *stress-driven* experiments. Significant differences in the hysteresis loops were found. The *strain-driven* curves show re-entrant behaviour (yield point) which is not observed in the *stress-driven* case. The dissipated energy in the *stress-driven* curves is larger than in the *strain-driven* ones. Results from recently proposed models qualitatively agree with experiments. We have extended one of these models in order to account for the driving-rate dependence of the dissipated energy.

PACS numbers: 81.30.Kf,75.60.Ej

Hysteresis is ubiquitous in many areas of physics. It is a signature of non-equilibrium effects and has attracted the attention of researchers from a long time and is still one of the most challenging subjects of research [1]. Typically, the phenomenon of hysteresis results in closed loops when plotting the external driving force *vs.* the generalized displacement (or vice versa).

Among hysteretic systems, particular attention has been devoted to athermal cases [2]. In these cases, hysteresis is not due to competition between the fast driving rate and slow thermal relaxation, but rather it originates from the existence of very high energy barriers that can only be overcome when the system reaches local marginal stability limits [3, 4]. The continuous change in the driving force results in discontinuous changes in the conjugate displacement, giving rise to avalanche dynamics. Such dynamics has been observed in a wide variety of ferroic materials such as ferromagnetic [5], ferroelectric [6] and martensitic [8] materials; field-driven vortex motion in type-II superconductors [7], and pressure-driven condensation of ⁴He on mesophorous solids [9], among others.

From an experimental point of view, it is usually easier to control the force while the conjugate displacement is measured. For instance, in magnetic systems, the magnetic field is readily controlled and magnetic flux is measured. Although more difficult, it has also been possible to control the magnetic flux [10] - which is suitable for studying materials displaying a rapid increase of magnetization. Moreover, the control of the amount of gas (generalized displacement) instead of the chemical potential has been shown to be the most convenient procedure in a number of gas adsorption experiments [11].

It has been customary to compare the hysteretic behaviour of different experimental systems without paying too much attention to which control variable is used. While for a macroscopic system in thermodynamic equilibrium both cases are equivalent because they are related by a Legendre transformation [12], it is not so obvious

that the hysteresis loops obtained when controlling the force will be similar to those obtained when the control parameter is the generalized displacement. Such a situation has been very recently theoretically studied [13, 14] by making use of the Random Field Ising Model (RFIM) [15], which is a prototype model for athermal hysteresis. Results predict significant differences in the hysteresis loops obtained in the force-driven case (external field H) to those obtained by driving the generalized displacement (magnetization M). It is the aim of the present Letter to address this issue from an experimental point of view.

Martensitic transitions (MT) offer a unique scenario to undertake such a task. A MT is a displacive first-order transition which involves a change in symmetry [16]. The transition can be induced by cooling but also by application of a mechanical stress. In this latter case, the driving force is the applied load, while the conjugate displacement is the elongation (or strain). Typical experiments are carried out using commercial tensile testing machines in which the control variable is the elongation, while the resulting force is measured by a load cell [17]. We have developed an experimental device which enables fine control of the applied force while the strain is monitored. In this Letter we present experiments performed on the same specimen using both kinds of driving mechanism. Results will enable direct comparison of the hysteresis loops obtained in the two cases for the same experimental system. Comparison with the predictions of recent theoretical approaches [13, 14] will be presented.

A Cu-Zn-Al single crystal was grown by the Bridgeman technique. The nominal composition was chosen so that the (athermal) MT on cooling without stress takes place from a cubic ($L2_1$) to a monoclinic ($18R$) structure slightly below room temperature ($T_M = 234K$). The actual composition, obtained from electron dispersion analysis is $Cu_{68.13}Zn_{15.74}Al_{16.13}$. A sample was mechanically machined from the ingot with cylindrical heads. The body of the sample has flat faces 35 mm long, 1.4 mm

thick and 3.95 mm width. The axis of the sample is close to the [001] crystallographic direction of the cubic phase. The sample was mechanically polished and then annealed for 20 min at 1073K, cooled in air down to room temperature and aged for 2 h in boiling water. This heat treatment ensures that the sample is in the ordered state, free from internal stresses and that the vacancy concentration is minimum at room temperature.

Special grips were machined that can be used in both experimental devices and adapt to the heads of the specimen. In the first device (from now on *strain-driven*), the control parameter is the elongation while the load is continuously monitored. The device is a commercial Instron 4302 tensile machine equipped with a cryofurnace. A second device (from now on *stress-driven*) was especially designed which enables control of the load applied to the sample while the elongation is continuously monitored. It has been adapted from that previously used by Carrillo et al. [18]. The upper grip is attached to a load cell hanging from the ceiling of the laboratory. Upper and lower ball-and-socket joints ensure good alignment. The lower grip holds a container that plays the role of a dead load. The load can be increased or decreased at a well-controlled rate by supplying or removing water by means of a pump. The strain is measured by a strain gauge attached to the sample. Since the stress needed to induce the MT is very sensitive to temperature, it is important to make sure that equivalent experiments are carried out at the same temperature. For this reason, the device is also designed so that the same cryofurnace can also be used. The cryofurnace enables a temperature control to within an accuracy of 0.1 K. In addition, in order to be able to compare the hysteresis loops obtained with the two devices, the same strain gauge was used in all experiments and the load cell of each set-up was calibrated using standard weights. For selected experiments at room temperature (without the cryofurnace), an optical microscope was incorporated into both devices, which enables *in situ* observations of microstructural changes. Fig. 1 shows typical results for the stress-strain curves obtained with the two devices. Upon increasing load, the parent cubic phase persists until it becomes unstable at a given value of the load, and the MT starts. Different hysteresis loops are observed in the two cases. Almost the entire *strain-driven* loop is enclosed within the *stress-driven* one which has a much larger area. In the *stress-driven* case, the stress slightly increases during the MT with an average slope that decreases as the driving rate is reduced. Extrapolation to zero rate still gives a finite (small) slope which can be caused by a weak concentration gradient along the axis of the sample. Different behaviour is observed in the *strain-driven* experiment. In this case, once the transition starts, the stress relaxes to a lower value (yield point effect) and then it weakly oscillates around an almost constant value as the MT progresses. For both driving modes, when the transition ends, a new reversible

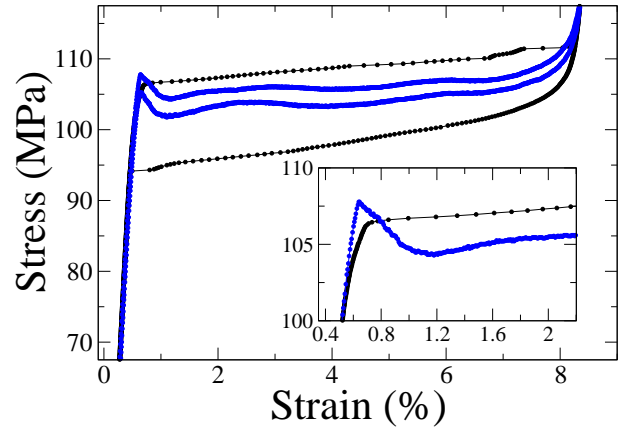


FIG. 1: (Color online) Experimental stress-strain hysteresis loop at 303.1 K in a Cu₆₈Zn₁₆Al₁₆ single crystal, obtained in strain-driven (squares) experiments at 0.005 mms⁻¹ and stress-driven (circles) experiments at 0.4 Ns⁻¹. The inset shows an enlarged view of the low-strain region.

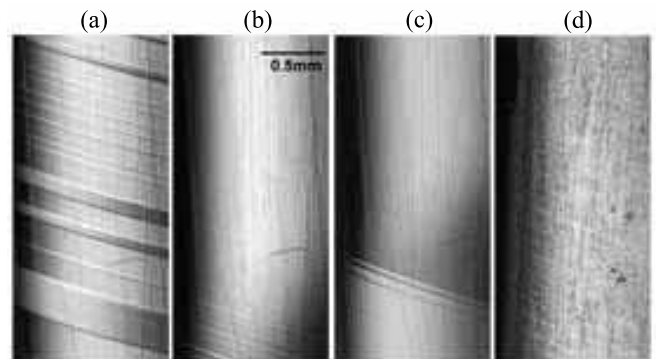


FIG. 2: Micrographs showing the microstructure at different stages of the MT: (a) 0.45%, (b) 0.48 % and (c) 0.57% strain. They illustrate the re-entrant behaviour in the *strain-driven* experiment. (d) 101.6 MPa, corresponds to the stress-driven case and illustrates nucleation of thin martensitic plates.

elastic regime in the martensitic phase is reached. Upon unloading, the behaviour parallels that observed in the loading branch, but with a certain amount of hysteresis. In particular for the *strain-driven* experiment, before the end of the reverse transition, there is an increase in the stress which reproduces the yield stress effect.

Optical observations have revealed significant differences in the early stages of the MT as shown in Fig. 2. The inset in Fig. 1 presents an enlarged view of the upper branch of the hysteresis loops on the low-strain region. The yield point in the *strain-driven* experiment is a consequence of re-entrant behaviour within the parent phase, associated with shrinkage and eventually the disappearance of previously formed martensitic plates. Such re-entrant behaviour is also observed on unloading, causing the yield point of the lower branch of the hystere-

sis loop. The evolution of the microstructure associated with this re-entrant behaviour is illustrated by the micrographs in Fig. 2 (a),(b) and (c). The existence of a yield point in conventional strain-driven experiments has also been reported for other martensitic alloys [19, 20]. Moreover, computer simulations of the mechanical response of a strain-driven martensitic system also show a yield point [21].

For the *stress-driven* experiment there is a deviation of the pure elastic behaviour well below the yield stress. This effect is due to the nucleation of a set of very thin martensitic plates all over the sample, as illustrated by the micrograph in Fig. 2(d). Interestingly, this is the only region where the *strain-driven* loop is outside the *stress-driven* one. For both driving mechanisms, steady state growth following the early stages is macroscopically similar, with parallel interfaces growing towards both ends of the specimen.

It is worth mentioning that the behaviour found in the present experiments for MT seems to be rather common in other systems. For instance, magnetization-driven magnetic hysteresis loops also show re-entrant behaviour [10] while no re-entrancy is present in magnetic field-driven loops. Furthermore, recent theoretical approaches and computer simulation studies for athermal plastic deformation [22] give curves with yield points when the control variable is the strain and without a yield point for the stress control variable. Interestingly, wiggling trajectories and re-entrance have even been reported to occur in displacement driven nanoscale systems such as deformation of gold nanowires [23] and RNA unfolding [24].

A relevant quantity in hysteretic systems is dissipated energy which is given by the area enclosed within the hysteresis loops. A noteworthy feature (see Fig. 1) is that the dissipated energy is much larger for the *stress-driven* case than for the *strain-driven* one. The dissipated energy is expected to depend on the driving rate of the control parameter. We have performed a series of experiments at different rates and the results of the area of the loops are plotted in Fig. 3 as a function of the rate. It is clear that the dissipated energy increases with increasing rate in both cases. Linear extrapolation to zero rate indicates non-vanishing hysteresis. It is important to note that even in the zero-rate limit, the dissipated energy for the *stress-driven* experiment is always larger than for the *strain-driven* case. We now discuss the experimental results presented here in relation to two recent approaches (in magnetic terminology) aimed at analysing *H*-driven and *M*-driven trajectories in the 3d-RFIM. Both models predict the existence of a yield point in the *M*-driven loop, which is caused by the absence of accessible states within a certain region of the *H* – *M* phase space in athermal systems [25]. Such a lack of accessible states results in different trajectories in the two driving mechanisms. For the *H*-driven case, this region is overcome by discontinuities in the generalized displacement. For the

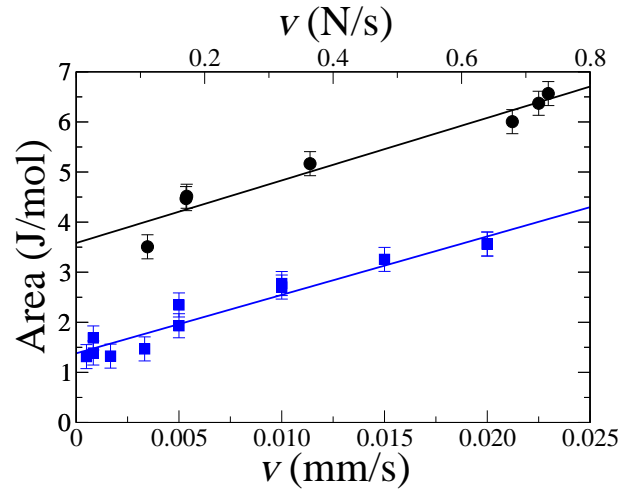


FIG. 3: (Color online) Area of the hysteresis loops as a function of the driving rate for the *stress-driven* case (circles) and the *strain-driven* case (squares).

M-driven case, the force is able to relax to lower values in such a way that the system adapts the trajectory to avoid these inaccessible states thus resulting in lower dissipation. Experimental data conform to this scenario except for the early nucleation stages. Actually, since the system is less constrained when driving the load (*H*-driven case in the model), nucleation can occur at lower values of the load since it can more freely adapt to the shape changes. Another result of models, is that both predict wiggling trajectories in the *M*-driven transition, reflecting the specific distribution of disorder in the system. This also agrees with experiments (see Fig. 1). One of the models [13] uses $T = 0$ adiabatic (infinitely slow) dynamics for the *M*-driven case which is the analogue of standard adiabatic dynamics introduced by Sethna et al. [15] in the *H*-driven case. The definition of the measured (output) field assumes that the external force instantaneously equals the highest value of the internal forces. Consequently, the *M*-driven loops have vanishing area. The strain-driven experiments presented here seem to indicate that although the area is quite small compared to the force-driven situation, after extrapolation to zero driving rate, a certain amount of dissipated energy still remains. With the aim of deepening the comparison of the model results with experimental ones, we have extended the $T = 0$ RFIM to incorporate the effect of a finite driving rate. For the *H*-driven case such an extension was proposed [26] by assuming an intrinsic average time for the avalanches τ_{av} to relax. In this case the finite-rate *H*-driven loops can be constructed from the adiabatic *H*-driven loops by considering the discontinuous step-like behaviour of the driving field with a certain ΔH in such a way that $\dot{H} = \Delta H/\tau_{av}$. This method allows the area of the loops in function of the driving rate

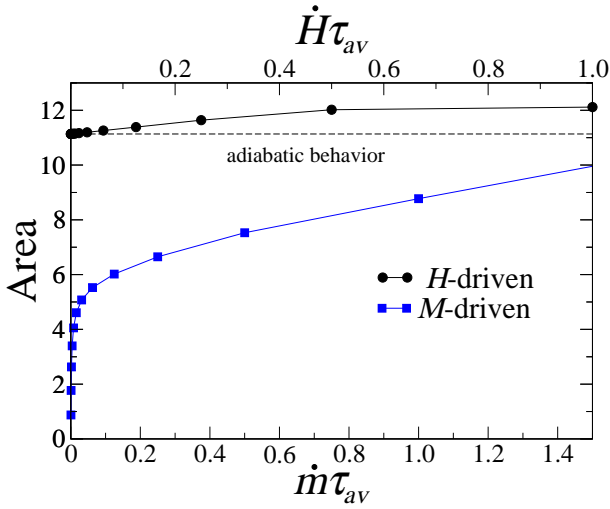


FIG. 4: (Color online) Area of the hysteresis loops as a function of the driving parameter rate (squares: stress-driven; circles: strain-driven) obtained by simulation of the $T=0$ RFIM.

to be computed. Results obtained for a cubic system with size $L = 20$ and standard deviation of the random-fields $\sigma = 1.0$ are shown in Fig. 4 (circles). Data correspond to averages over more than 1000 realizations of the random fields. We have considered a similar definition in the simulations of finite-rate M -driven systems. It is assumed that the force is only able to relax at given values of the magnetization which are separated by Δm so that $\dot{m} = \Delta m/\tau_{av}$. An example of the obtained results for the same system is also shown in Fig. 4 (squares). It is remarkable that results from numerical simulations satisfactorily reproduce the major features found experimentally, i.e. an increase in dissipation with increasing rate, and the fact that the dissipated energy is always larger for the force-driven cases. Only at low rate limit, do numerical data show the already mentioned tendency towards a vanishing area. Such a tendency is due to the assumption of the infinitely fast response of the system assumed in the models and therefore it is not corroborated by experimental data. As shown in Fig. 4, finite-rate models indicate that dissipation in the large-rate limit of the M -driven dynamics will reach the zero-rate (adiabatic) limit of the H -driven case, as indicated by the dashed line in Fig. 4. Although not conclusively, experimental data (Fig. 3) seem to be consistent with such a prediction.

To conclude, we have experimentally shown that metastable trajectories exhibit a strong dependence on the driving mechanism in martensitic materials; the displacement driven loops exhibit yield point and lower dissipation. Results conform to recent theoretical predictions for athermal systems. It is expected that the reported features will be common to many hysteretic systems undergoing first-order phase transitions.

This work has received financial support from CICYT

(Spain), project MAT2004-1291, CIRIT (Catalonia), project 2005SGR00969, and Marie-Curie RTN MULTIMAT (EU), contract MRTN-CT-2004-5052226. R. Romero acknowledges a grant from Secretaría de Estado de Universidades e Investigación (Spain). The authors acknowledge F.J. Pérez-Reche, M. Ahlers, T. Lookman, A. Saxena, M.L. Rosinberg for fruitful discussions and =Toscano for experimental assistance.

* Electronic address: eduard@ecm.ub.es

- [1] *The Science of Hysteresis*, G. Bertotti and I. Myeroyz eds., Academic Press, 2005.
- [2] J.P. Sethna, K.A. Dahmen, O. Perkovic, in *The Science of Hysteresis*, G. Bertotti and I. Myeroyz eds., Academic Press, 2005.
- [3] W. Cao, J.A. Krumhansl, R.J. Gooding, Phys. Rev. B **41**, 11319 (1990).
- [4] F.J. Pérez-Reche, E. Vives, L. Mañosa, A. Planes, Phys. Rev. Lett. **87**, 195701 (2001).
- [5] E. Puppin, Phys. Rev. Lett. **84**, 5415 (2000).
- [6] E.V. Colla, L.K. Chao and M.B. Weissman, Phys. Rev. Lett. **88**, 017601 (2002); B. Tadic, Eur. Phys. J. **28**, 81 (2002).
- [7] E. Altshuler and T.H. Johansen, Rev. Mod. Phys. **76**, 471 (2004).
- [8] E. Vives et al. Phys. Rev. Lett. **72**, 1694 (1994).
- [9] M.P. Lilly, P.T. Finley, R.B. Hallock, Phys. Rev. Lett. **71**, 4186 (1993).
- [10] W. Grosse-Nobis, J. Magn. Magn. Mat. **4**, 247 (1977).
- [11] A.P.Y. Wong, M.H.W. Chan, Phys. Rev. Lett. **65**, 2567 (1990).
- [12] K. Huang, *Statistical Mechanics, 2nd edition*, John Wiley and Sons, New York 1987.
- [13] X. Illa, M.L. Rosinberg, P. Shukla, E. Vives, Phys. Rev. B **74**, 224404 (2006).
- [14] X. Illa, M.L. Rosinberg, E. Vives, Phys. Rev. B. **74**, 224403 (2006).
- [15] J.P. Sethna et al., Phys. Rev. Lett **70** 3347 (1993).
- [16] Z. Nishiyama, *Martensitic Transformations*, Academic Press, New York 1978.
- [17] There are tensile machines which enable the load to be controlled instead of the displacement by making use of a feedback procedure. However, since the MT occurs very rapidly (typically at the speed of sound) the feedback does not ensure a constant load rate at all times.
- [18] L. Carrillo, J. Ortín, Phys. Rev. B **56**, 11508 (1997).
- [19] M. Landa, V. Novák, P. Sedlák, P. Sittner, Ultrasonics **42**, 519 (2004).
- [20] M.A. Iadicola, J.A. Shaw, Int. J. Plast. **20**, 577 (2004).
- [21] R. Ahluwalia, T. Lookman, A. Saxena, Acta Mater. **54**, 2109 (2006).
- [22] E. Bouchbinder, J.S. Langer, I. Procaccia, arXiv:cond-mat/0611025 and 0611206.
- [23] G. Rubio-Bollinger et al., Phys. Rev. Lett. **87**, 026101 (2001).
- [24] M. Manosas and F. Ritort, Biophys. Jour. **88**, 3224 (2005).
- [25] F. Detcheverry, M.L. Rosinberg, G. Tarjus, Eur. Phys. J. B **44**, 327 (2005).

[26] F.J.Pérez-Reche *et al.*, Phys. Rev. Lett. **93**, 195701 (2004).